ELSEVIER

Journal of Alloys and Compounds 253–254 (1997) 609–612

Journal of ALLOYS AND COMPOUNDS

Correlation between crystal structure and electrochemical properties of C14 Laves-phase alloys

H. Nakano[a,*], S. Wakao[b], T. Shimizu[c]

[a]*School of High-Technology for Human Welfare, Tokai University, 317 Nishino, Numazu, Shizuoka, 410-03, Japan*
[b]*Tokai University, 3-10-22 Daita, Setagaya, Tokyo, 155, Japan*
[c]*Daido Steel Co., Ltd., 2-30 Daido, Minami, Nagoya, 457, Japan*

Abstract

By examining the relationships between the structure and the thermodynamic and electrochemical properties for $Zr_{1-x}Ti_x(V_{0.1}Mn_aNi_bE_c)_\alpha$ (x=0.1–0.3, a=0.28–0.30, b=0.50–0.57, c=0.05–0.12, α=1.6–1.8, E=Co, Fe, Mo) alloy system with C14 type structure, the following results were obtained. The partial molar enthalpy for hydride formation decreases linearly with decreasing cell volume V_{C14} of the C14 phase. This means that the hydride becomes unstable with decreasing V_{C14}, as is the case for the C15 type structure. Both $-\Delta H$ and V_{C14} decrease with decreasing average atomic radius of the alloy, and the correlation coefficient was sufficiently high for each value. The discharge capacity and dischargeability also depend on $-\Delta H$ and V_{C14}.

Keywords: Laves-phase; C14 crystal structure; Hydrogen-absorbing alloy; Hydride electrode

1. Introduction

Laves-phase AB_2 alloys have attracted attention as negative electrodes of rechargeable Ni–MH batteries because of their large capacity of about 370–410 $mAhg^{-1}$. Many studies have been conducted on these alloy electrodes with the object of improving their electrochemical performance and durability [1–7].

It is basically important in alloy-designing to investigate the correlation between the structural and electrochemical properties. In the rare-earth–nickel AB_5 type alloys, it has been reported that the free energy change ΔG, the enthalpy change ΔH for hydride formation, and the equilibrium hydrogen pressure all depend on cell volumes [8–12]. On the other hand, in the case of pseudo-binary Laves-phase AB_2 alloys with C15 structure, the linear correlation between ΔH and cell volume V_{C15} has been confirmed both experimentally [4,5] and theoretically on the basis of thermodynamic considerations [15]. Moreover, it is noted that ΔH and V_{C15} depend on the average atomic radius r_{av} and average electronegativity of the alloy's constituent elements [4,5].

In this study, electrochemical and thermodynamic properties such as charge–discharge capacity, dischargeability, and ΔH were measured for Zr-Ti-V-Mn-Ni-E (Co, Fe, Mo) alloys with C14 structure. The correlations between their electrochemical properties, ΔH, cell volume, and alloy r_{av} are also discussed.

2. Experimental details

Some eighteen alloy samples of AB_2 type were investigated as shown in Table 1. Their composition range was as follows: $Zr_{1-x}Ti_x(V_{0.1}Mn_aNi_bE_c)_\alpha$, (E=Co, Fe, Mo, x= 0.1–0.3, a=0.28–0.30, b=0.50–0.57, c=0.05–0.12, 0.1+ $a+b+c$=1.0, α=1.6–1.8). This formula implies that Zr and Ti, being the larger atoms, occupy the A-lattice site in the AB_2 crystal structure and the other elements, being the smaller atoms, the B-lattice site. However, this assumption needs to be proved by structural analysis.

The alloys were prepared in amounts of about 50 g by arc-melting in an argon atmosphere and treated at 1080°C for 10 h in vacuum. Their exact compositions and crystal structures were determined by elemental analysis and X-ray powder diffraction analysis, respectively. The abundance of the C14 phase was calculated by using the peak intensity obtained from the ASTM cards and the measured peak intensity of the (103) and (201) reflections which

*Corresponding author.

0925-8388/97/$17.00
PII S0925-8388(96)03089-7

Table 1
Electrochemical properties, enthalpy change (ΔH), cell volume (V_{C14}), abundance (R_{C14}) of C14, ratio (r_A/r_B) of atomic radii of A and B atoms and average atomic radius (r_{av})

No.	Alloy	C_H^{*a}	DC ($mAhg^{-1}$)			D/C (%)	$-\Delta H^{*b}$	V_{C14} (Å)	R_{C14} (%)	r_A/r_B^{*c}	r_{av} (Å)
			17	55	110						
1	$Zr_{0.9}Ti_{0.1}(V_{0.10}Mn_{0.28}Ni_{0.57}Mo_{0.05})_{1.6}$	464	256	198	145	55.1	50.06	181.63	100	1.1995	1.4111
2	$Zr_{0.8}Ti_{0.2}(V_{0.10}Mn_{0.28}Ni_{0.57}Fe_{0.05})_{1.6}$	457	366	315	243	80.1	43.98	177.70	100	1.1964	1.4018
3	$Zr_{0.8}Ti_{0.2}(V_{0.10}Mn_{0.28}Ni_{0.57}Co_{0.05})_{1.6}$	458	370	326	276	80.8	43.20	177.23	100	1.1968	1.4015
4	$Zr_{0.8}Ti_{0.2}(V_{0.10}Mn_{0.28}Ni_{0.57}Mo_{0.05})_{1.6}$	466	329	212	145	70.6	47.59	180.11	100	1.1905	1.4061
5	$Zr_{0.8}Ti_{0.2}(V_{0.10}Mn_{0.28}Ni_{0.57}Mo_{0.05})_{1.7}$	452	380	319	238	84.1	45.86	178.68	100	1.1958	1.4022
6	$Zr_{0.7}Ti_{0.3}(V_{0.10}Mn_{0.28}Ni_{0.57}Fe_{0.05})_{1.6}$	461	395	297	187	85.7	43.06	176.73	100	1.1874	1.3968
7	$Zr_{0.7}Ti_{0.3}(V_{0.10}Mn_{0.28}Ni_{0.57}Co_{0.05})_{1.6}$	445	383	302	210	86.1	41.81	175.98	92	1.1878	1.3965
8	$Zr_{0.7}Ti_{0.3}(V_{0.10}Mn_{0.28}Ni_{0.57}Mo_{0.05})_{1.6}$	459	371	250	172	80.8	46.20	177.96	100	1.1816	1.4011
9	$Zr_{0.7}Ti_{0.3}(V_{0.10}Mn_{0.28}Ni_{0.57}Fe_{0.05})_{1.7}$	449	422	374	285	94.0	39.56	174.82	72	1.1926	1.3930
10	$Zr_{0.7}Ti_{0.3}(V_{0.10}Mn_{0.28}Ni_{0.57}Co_{0.05})_{1.7}$	426	400	382	359	93.9	39.55	174.33	92	1.1930	1.3926
11	$Zr_{0.7}Ti_{0.3}(V_{0.10}Mn_{0.28}Ni_{0.57}Mo_{0.05})_{1.7}$	453	395	284	200	87.2	43.45	176.98	100	1.1866	1.3974
12	$Zr_{0.7}Ti_{0.3}(V_{0.10}Mn_{0.28}Ni_{0.57}Fe_{0.05})_{1.8}$	443	415	397	380	93.7	38.58	173.63	92	1.1974	1.3894
13	$Zr_{0.7}Ti_{0.3}(V_{0.10}Mn_{0.28}Ni_{0.57}Co_{0.05})_{1.8}$	444	418	390	372	94.1	38.70	173.87	71	1.1979	1.3891
14	$Zr_{0.7}Ti_{0.3}(V_{0.10}Mn_{0.28}Ni_{0.57}Mo_{0.05})_{1.8}$	449	423	390	348	94.2	41.57	175.75	84	1.1913	1.3939
15	$Zr_{0.7}Ti_{0.3}(V_{0.10}Mn_{0.30}Ni_{0.53}Fe_{0.05}Mo_{0.02})_{1.6}$	475	314	160	86	66.1	46.67	178.00	100	1.1829	1.4001
16	$Zr_{0.7}Ti_{0.3}(V_{0.10}Mn_{0.28}Ni_{0.50}Fe_{0.08}Mo_{0.04})_{1.6}$	464	178	74	-	38.4	45.47	178.40	76	1.1822	1.4006
17	$Zr_{0.7}Ti_{0.3}(V_{0.10}Mn_{0.30}Ni_{0.53}Fe_{0.05}Mo_{0.02})_{1.7}$	464	393	273	155	84.7	41.06	176.00	100	1.1880	1.3964
18	$Zr_{0.7}Ti_{0.3}(V_{0.10}Mn_{0.28}Ni_{0.50}Fe_{0.08}Mo_{0.04})_{1.7}$	449	240	130	53	53.5	44.70	177.21	100	1.1872	1.3969

C_H, first charged hydrogen content ($mAhg^{-1}$) at 17 mAg^{-1}; DC, discharge capacity; D/C, dischargeability; *[a], mAg^{-1}; *[b], kJ mol H_2^{-1}; *[c], r_{av} were calculated from the metallic bond radii (Zr = 1.60, Ti = 1.47, V = 1.35, Mn = 1.37, Ni = 1.25, Co = 1.25, Fe = 1.26, Mo = 1.40 Å).

characterize the C14 structure as shown in previous studies [4,5].

In order to calculate the atomic radius ratio for $AB_{2-\alpha}$, the authors assumed that vacancies are absent and that $\alpha/3$ of A atom migrate to B atom sites although this might not be justified because vacancies were shown to exist from density measurement. Consequently, the formula $AB_{2-\alpha}$ can be rewritten as follows.

$$AB_{2-\alpha} \rightarrow A_{(1-\alpha/3)}(B_{(2-\alpha)}A_{\alpha/3}) \rightarrow A(B_xA_y)_{2.0}$$

$$[x = 3(2-\alpha)/\{2(3-\alpha)\},\ y = \alpha/\{2(3-\alpha)\}].$$

The atomic radius ratio was calculated from the above formula. The values shown in Table 1 were calculated by assuming that both Zr and Ti atoms migrate, but the ratio increased by a maximum of 2.2% by assuming the migration of Ti atoms only except for No. 1 alloy.

An electrode of a disk type shape was made by mixing the alloy powder (200–350 meshes, 24 wt.%), Ni powder (72 wt.%), and PTFE powder (polytetrafluoroethylene, 4 wt.%), and molding under a pressure of 780 MPa for 15 min. It had a diameter of 13 mm and a thickness of approximately 1.0 mm. A lead wire was attached to one side of the pellet [4]. Charge–discharge was performed on the opposite side.

The electrodes were charged at a current density of 17 mAg^{-1} after immersion in 6 M KOH for 15 h. The hydrogen gas generated during charging was collected in a gas burette. The electrochemically absorbed hydrogen contents of the alloy were calculated by subtracting the quantity of electricity required for the hydrogen gas evolution from the total integrated quantity of electricity. The alloy electrodes were discharged to −0.6 V vs. Hg/HgO at current densities of 17–110 mAg^{-1} for measurement of discharge capacity. The operating temperature was kept at a constant 25°C in the charge–discharge processes.

The thermodynamic quantities, such as the partial molar enthalpy of the hydride formation, were obtained at about the half-point of discharge capacity at 17 mAg^{-1} (H/M = 0.55–0.85) on the basis of the temperature change of the equilibrium electrode potential as described in Refs. [14,15].

3. Results and discussion

3.1. Crystal structure

For the Laves-phase in the Zr-Ti-V-Ni system it was reported [13] that the C14 structure predominated when the ratio r_A/r_B of the atomic radii of the A and B atoms was less than 1.225. For bigger values the C15 structure predominated. For the alloys examined in this study, the r_A/r_B values are in the range of 1.18 to 1.20. As expected, X-ray diffraction results indicate that most of the alloys were C14 single phase and some contained additional C15 phase. Small amounts of α-Zr phase were also present in the cases of $AB_{1.6}$ alloys.

The cell volumes V_{C14} as calculated from the lattice constants (a, c) of the C14 structure by using Eq. (1) ranged from 173.63 to 181.63 $Å^3$ as shown in Table 1.

$$V_{C14} = \sqrt{3}a^2c/2 \quad (1)$$

3.2. ΔH and cell volume V_{C14}

The partial molar enthalpy ΔH for hydride formation was measured electrochemically and found to range from 38.6 to 50.1 kJ mol H_2^{-1} (Table 1). As indicated in Fig. 1 and Eq. (2), $-\Delta H$ was highly correlated with V_{C14}.

$$-\Delta H = 1.511 V_{C14} - 224.0 \quad \text{(correlation coefficient } R = 0.978) \qquad (2)$$

That is, $-\Delta H$, which expresses the stability–instability of the absorbed hydrogen in the alloy, decreased with decreasing V_{C14} in this C14 alloy series, similarly to the C15 series [4,5].

On the other hand, V_{C14} decreases in accordance with the decrease of r_{av} as defined by Eq. (3). This correlation is shown in Eq. (4).

$$r_{av} = \sum (a_i r_i) \Big/ \sum a_i \qquad (3)$$

$$V_{C14} = 366.6 r_{av} - 335.6 \quad (R = 0.978) \qquad (4)$$

From Eqs. (2) and (4), the correlation between $-\Delta H$ and r_{av} was expressed by Eq. (5).

$$-\Delta H = 542.8 r_{av} - 715.5 \quad (R = 0.937) \qquad (5)$$

For the present C14 alloys it can be concluded that r_{av} is a factor that governs $-\Delta H$ and V_{C14}. This result differs from the case of C15 alloys [4,5].

3.3. Electrochemical properties

The electrochemical properties, such as the electrical capacity charged initially at 17 mAg^{-1}, the discharge capacities at current densities 17–110 mAg^{-1}, and the dischargeabilities indicating the ratio of discharge capacities at 17 mAg^{-1} and charged hydrogen contents are shown in Table 1.

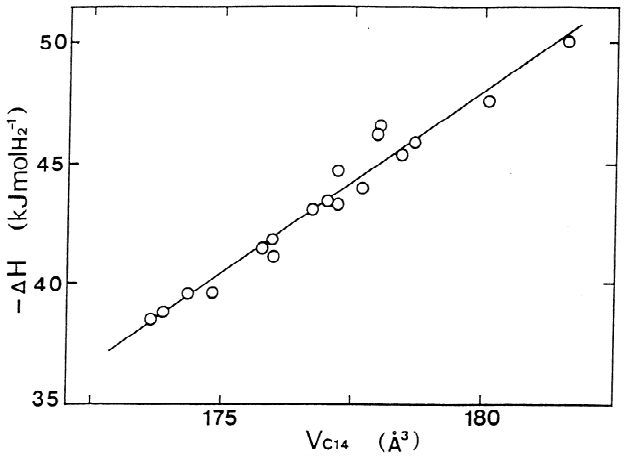

Fig. 1. Correlation between cell volume V_{C14} and $-\Delta H$.

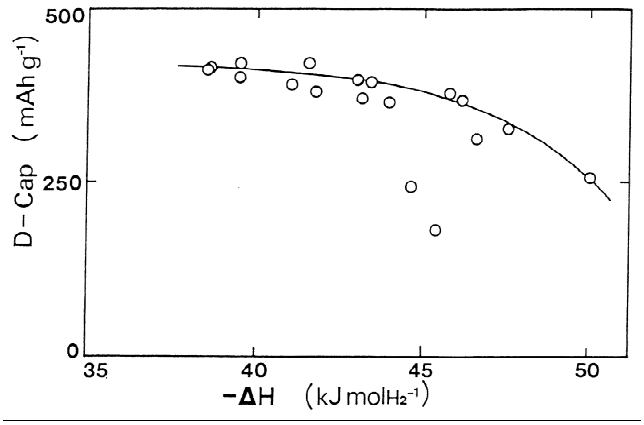

Fig. 2. Correlation between $-\Delta H$ and discharge capacity DC at 17 mAg^{-1}.

Most of the alloy electrodes examined were easily charged to their maximal hydrogen contents. The hydrogen contents during the first charge were in the range of 426–475 $mAhg^{-1}$.

For many alloy electrodes, the discharge capacities at 17 mAg^{-1} were greater than 80% of the initially charged hydrogen contents, typically more than 370 $mAhg^{-1}$. The discharge capacities tend to decrease with increasing $-\Delta H$ (Fig. 2). In the case of $Zr_{0.7}Ti_{0.3}(V_{0.10}Mn_{0.28}Ni_{0.57}Fe_{0.05})_{1.8}$ (No. 12) having $-\Delta H = 38.6$ kJ mol H_2^{-1}, the discharge capacity was 415 $mAhg^{-1}$ at 17 mAg^{-1}, and remained at 380 $mAhg^{-1}$ at 110 mAg^{-1}.

The discharge capacity and dischargeability for high-rate discharge may be superior in alloys having an appropriately smaller $-\Delta H$ value than in this example. An estimate of the $-\Delta H$ and V_{C14} values referring to basic properties of the alloy is important for alloy-designing. The above-mentioned contribution of r_{av} will be useful in such designing.

4. Conclusions

The following correlations were found between cell volume, ΔH and electrochemical properties of the Laves-phase alloys Zr-Ti-V-Mn-Ni-E (Co, Fe, Mo) with C14 structure.

(1) The $-\Delta H$ values decrease linearly with decreasing cell volume V_{C14}.
(2) $-\Delta H$ and V_{C14} decrease with decreasing average atomic radius r_{av}.
(3) The discharge capacity and the dischargeability depend on $-\Delta H$ and V_{C14}.

References

[1] J. Huot, E. Akiba, T. Ogura and Y. Ishido, J. Alloys Comp., 218 (1995) 101.
[2] A. Zuttel, F. Meli and L. Schlapbach, J. Alloys Comp., 231 (1995) 645.
[3] J.Y. Yu, Y.Q. Lei, C.P. Chen, J. Wu and Q.D. Wang, J. Alloys Comp., 231 (1995) 578.
[4] H. Nakano and S. Wakao, J. Alloys Comp., 231 (1995) 587.
[5] H. Nakano, I. Wada and S. Wakao, Denki Kagaku, 62 (1994) 953.
[6] S.R. Ovshinsky, J.A. Fetcenko and J. Ross, Science, 260 (1993) 176.
[7] H. Miyamura, T. Sakai, N. Kuriyama, K. Oguro, A. Kato and H. Ishikawa, Proc. of the Symp. on Hydrogen Storage Materials, Batteries, and Electrochemistry, Arizona, Oct. 14–17, 1991, Electrochemical Society, Pennington, NJ, 92(5) (1992), 179.
[8] D.G. Westlake, J. Less-Comm. Metals, 91 (1983) 1.
[9] C.E. Lundin, F.E. Lynch and C.B. Magee, J. Less-Comm. Metals, 56 (1977) 19.
[10] D.M. Gruen, M.H. Mendelsohn and I. Sheft, Proc. Symp. on Electrode Materials and Processes for Energy Conversion and Storage, Philadelphia, May 8–13, 1977, Electrochemical Society, Princeton, NJ, 1977, pp. 482–485.
[11] M.H. Mendelsohn, D.M. Gruen and A.E. Dwight, Nature, 269 (1977) 45.
[12] K.H.J. Buschow and A.R. Miedema, Proc. Int. Symp. on Hydride for Energy Storage, Geilo, August, 1977, Pergamon, Oxford, 1978, p. 235.
[13] H. Nakano, I. Wada and S. Wakao, J. Adv. Sci., 4 (1992) 239.
[14] S. Wakao and Y. Yonemura, J. Less-Comm. Metals, 89 (1983) 481.
[15] H. Sawa and S. Wakao, Mater. Trans. JIM, 31 (1990) 487.